ACS Medicinal Chemistry Letters

LETTER

pubs.acs.org/acsmedchemlett

Synthesis and Cardiac Imaging of ^{18}F-Ligands Selective for β_1-Adrenoreceptors

Heike S. Radeke,* Ajay Purohit, Thomas D. Harris, Kelley Hanson, Reinaldo Jones, Carol Hu, Padmaja Yalamanchili, Megan Hayes, Ming Yu, Mary Guaraldi, Mikhail Kagan, Michael Azure, Michael Cdebaca, Simon Robinson, and David Casebier

Research and Development, Lantheus Medical Imaging, 331 Treble Cove Road, North Billerica, Massachusetts 01862, United States

Supporting Information

ABSTRACT: A series of potent and selective β_1-adrenoreceptor ligands were identified (IC_{50} range, 0.04−0.25 nM; β_1/β_2 selectivity range, 65−450-fold), labeled with the PET radioisotope fluorine-18 and evaluated in normal Sprague−Dawley rats. Tissue distribution studies demonstrated uptake of each radiotracers from the blood pool into the myocardium (0.48−0.62% ID/g), lung (0.63−0.97% ID/g), and liver (1.03−1.14% ID/g). Dynamic μPET imaging confirmed the in vivo dissection studies.

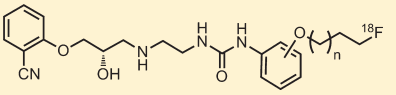

KEYWORDS: PET, β_1-selective ligand, cardiac imaging, heart failure, ^{18}F-labeling

The β_1- and β_2-adrenoreceptors (β-AR) play an important role in the regulation of heart function and have been extensively studied in recent decades,[1,2] as changes in the number and ratio of cardiac β-ARs have been associated with several diseases of the heart including myocardial ischemia,[3] congestive heart failure,[4] cardiomyopathy,[5] and hypertention.[6] In the healthy human heart, β_1-AR is the dominant subtype (4:1 ratio, β_1:β_2-AR) and widely distributed. However, in the failing heart, a predictable decrease in cardiac β_1-AR density (3:2 ratio, β_1:β_2-AR density observed in heart tissue of postmortem heart failure patients), coupled with enhanced sympathetic activity, boosting cardiac-derived noradrenaline and adrenaline levels, leads to further desensitization and subsequent down-regulation of β_1-ARs as well as a decrease in cardiac contractility, the hallmark of heart failure.[7] In addition, it has been shown that β_1-AR down-regulation precedes clinical heart failure and may indeed be an early clinical marker of left ventricular dysfunction.[8]

To date, the human heart has been extensively studied with positron emission tomography (PET) and single photon emission computed tomography (SPECT) to assess myocardial blood flow and substrate metabolism.[9] However, these imaging techniques have yet to realize the opportunity of noninvasive assessment of cardiac AR density, distribution, and occupancy using endogenous ligands or drugs,[10] where the capacity of PET to be used for repeat measurements may significantly aid in monitoring and treatment of various heart diseases.[11] Identification of the population at risk for developing heart failure before clinical symptoms are noticed would greatly improve patient management as well as the stratification of a patient population that would benefit from placement of an implantable cardioverter-defibrillator (ICD).[12]

At present, however, no optimal radioligands for imaging cardiac β_1-AR using SPECT or PET are available,[13] where the most extensively studied tracer in cardiovascular disease patients is the nonselective ligand [^{11}C]CGP-12177.[14] Regrettably, its demonstrated capacity for visualization and quantification of β-AR density alone rather than the β_1-AR population specifically is less valuable for assessment of cardiac diseases.[15]

In contrast, the β_1-AR selective antagonist ICI 89,406 (**1**; Scheme 1) has previously been shown to produce effective blockage of β_1-AR during exercise in patients with angina pectoris.[16] As such, Schaefer et al. chose this compound as their lead structure in the development of new β_1-AR selective ligands for PET and SPECT.[17−19] Notably, the authors developed an *O*-methyl derivative of **1**, labeled with carbon-11 ([^{11}C]OMe-ICI 89,406; [^{11}C]**2**), that exhibited high affinity and selectivity for β_1-AR in vitro. Unfortunately, in vivo studies did not demonstrate high specific binding to myocardial β_1-AR; rapid metabolism and high nonspecific binding in the myocardium were observed.[20]

Our goal in the present study was to expand on the known structure−activity profile of **1** and evaluate multiple ^{18}F-labeled derivatives through in vivo imaging studies.[21,22] Traditionally, ICI 89,406 along with a very small set of nonfluorinated derivatives were prepared via the acid-catalyzed epoxide opening of (*S*)-(oxiran-2-ylmethoxy)benzonitrile with an appropriately functionalized amine (Scheme 1).[19] The various fluorinated β_1-ligands prepared in our study took advantage of this synthetic disconnection approach, where several functionalized amines were first prepared and then exposed to a series of substituted (*S*)-(oxiran-2-ylmethoxy)benzonitriles to create a diverse set of compounds with A and B regions as shown in Chart 1.

In conjunction, two complementary synthetic strategies were developed to generate the requisite functionalized amino-urea derivatives. Within each analogue, the central urea linkage was constructed through condensation of *tert*-butyl-2-aminoethylcarbamate with either a commercially available isocyanate or an

Received: October 11, 2010
Accepted: July 22, 2011
Published: July 22, 2011

in situ-generated *p*-nitrophenylcarbamate (Schemes 2 and 3 and Supporting Information).

In certain cases, additional functional group manipulations were required to complete the construct prior to reaction with the substituted (*S*)-(oxiran-2-ylmethoxy)benzonitriles, while in others, simple deprotection of the derived urea remained to generate the requisite coupling partner.[23]

To generate multiple radioligands more efficiently, the radiosynthetic procedure that we chose for labeling compounds **5**−**7** utilized a well-established, two-step process that allows for labeling of multiple phenolic precursors with various ^{18}F-labeled alkyl substituents (Scheme 4).[24] A robotic radiosynthesis station, which can conduct multistep radiosynthetic procedures, was developed and evaluated with our selected precursor phenols.

Scheme 1. Synthesis of ICI 89, 406, and Analogues[a]

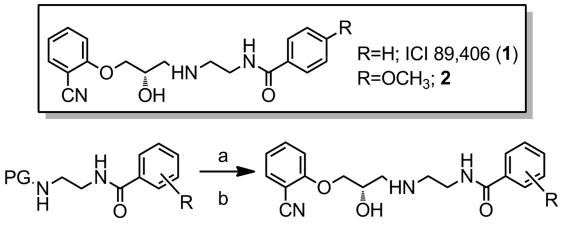

[a] Reagents and conditions: (a) HCl, dioxane, or TFA, CH_2Cl_2, 55−98%. (b) MeCN or *i*-PrOH, *i*-Pr_2NEt, Et_2BOMe, Yb(OTf)$_3$, 43−45%; method A, B, or C, 10−45%.

For preparation of the conjugate ^{18}F-labeled alkylfluorides, precursor materials were required that contain activated leaving groups such as sulfonate esters (e.g., tosylates, mesylate). Primary derivatives were preferred because of their ease of displacement with fluorine-18 as compared to secondary derivatives, which often eliminate under the basic fluorination conditions. With these caveats in mind, we first generated the ^{18}F-labeled radioligands [^{18}F]fluoroethyl-(**41**) and [^{18}F]fluoropropyl tosylate (**62**) from their respective bis-tosylate precursors using a combination of published methods.[25] Subsequent reaction of **41** and **62** with phenol precursors **47** or **49** under standard Williamson conditions afforded [^{18}F]**5**−**7** after high-performance liquid chromatography (HPLC) purification (11−31% conversion after 30 min; see the Supporting Information for details). Notably, for each radiotracer, ∼25 mCi of the final compound was isolated from ∼500 mCi of [^{18}F]NaF in high radiochemical purity; the total synthesis time was 120 min. Specific activity values ranged from 750 to 2000 mCi/μmol depending upon the final radioactive concentration. Significantly, the single-step labeling process, ([^{18}F]KF, K_{222}, MeCN, 90 °C, 15 min), using the derivative tosylate precursors of [^{18}F]**5**−**7**, demonstrated rather poor chemical efficiency (<2% radiochemical yield).

Initial synthetic efforts were directed toward introduction of a fluorine atom into the B region of **1** (Table 1). Importantly, the aromatic fluorides **3** and **4** both exhibited potent β_1-AR binding activity (IC_{50} = 0.2 and 0.1 nM, respectively) and β_1/β_2-AR selectivity (69- and 150-fold, respectively), revealing a modest preference for locating fluorine at the para-position of the

Chart 1. Diverse Moieties for the A and B Region Linked via the ICI 89,406 Backbone

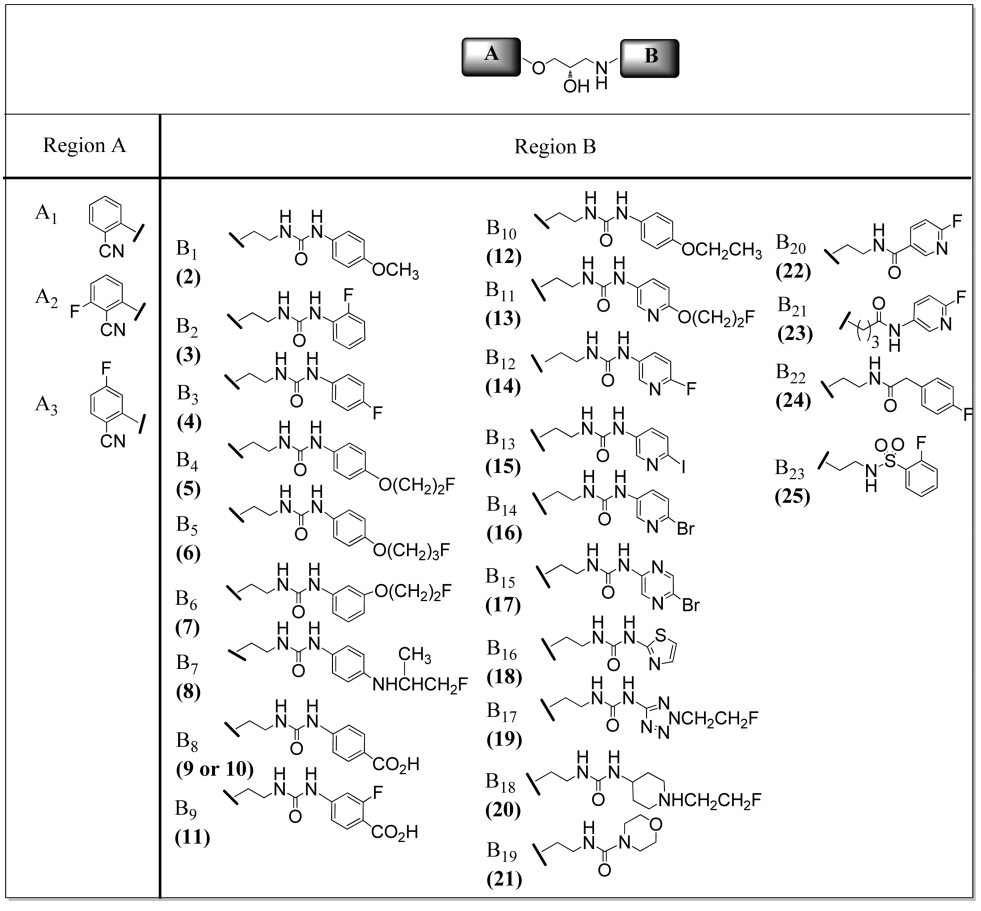

dx.doi.org/10.1021/ml1002458 |*ACS Med. Chem. Lett.* 2011, 2, 650–655

Scheme 2[a]

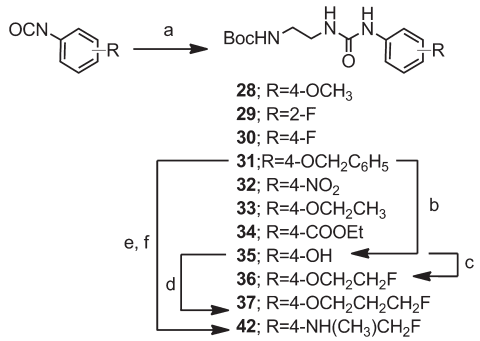

[a] Reagents and conditions: (a) *tert*-Butyl-2-aminoethylcarbamate, THF, 0 °C, 2.5−16 h, 47−93%. (b) H_2, Pd/C, EtOH, 12 h, 91%. (c) 2-Fluoroethanol, diisopropyl azodicarboxylate, PPh_3, THF, 5 h, 20%. (d) 3-Fluoropropyl tosylate, NaOH, DMSO, 75 °C, 30 min, 71%. (e) Pd/C, H_2, MeOH. (f) Fluoroacetone, $NaBH(OAc)_3$, THF.

Scheme 3. Synthesis of Carbamates 38, 40, 51−60, 63, and 65[a]

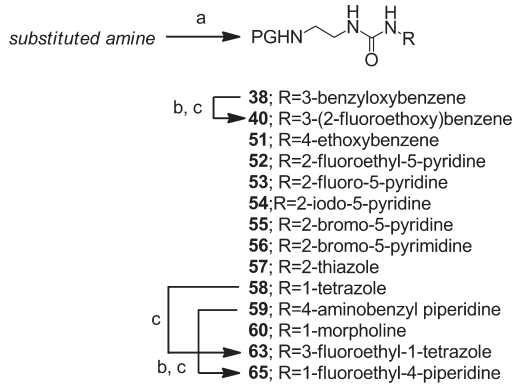

[a] PG (protecting group) = Boc or Cbz. Reagents and conditions: (a) (i) 4-Nitrophenyl chloroformate, pyridine, solvent, overnight; (ii) NBoc-ethylenediamine, base, DMF or THF, 15 min −2 h, 29−94%. (b) H_2, Pd/C, EtOH, 90−96%. (c) 2-Fluoroethyl tosylate, K_2CO_3, DMF, 50−80 °C, 2−24 h, 42−96%.

aromatic ring. Alternatively, extension of the methoxy function in **2** to fluoroethoxy derivative **5** resulted in a 3-fold increase in selectivity while maintaining β_1-AR binding potency.[26] Interestingly, further extension to yield a fluoropropoxy function (**6**) resulted in decreased β_1-AR binding potency and subtype selectivity as compared to **2**. Maintaining the fluoroethoxy group in **5** with transposition to the meta-position did, however, improve β_1-AR potency albeit with reduced selectivity (e.g., **5** and **7**, Table 1). Relocating the fluorine atom from the B region (**5**) to the A region as in **12** induced a marked decrease in β_1-AR potency and selectivity. Lastly, when the fluoroethoxy group was replaced with a fluorinated amino derivative, β_1-AR potency and selectivity significantly decreased (**8**). Taken together, fluorine substitution was better tolerated on the B ring with regard to both β_1-AR potency and selectivity.

Previous studies have identified potent β_1-AR selective ICI 89,406 analogues, which contain a carboxylic acid residue in the para-position of the B ring.[27] Hence, a set of fluorinated analogues (**9**−**11**), which contain a related substitution pattern, were prepared. Compounds **9** and **10** exhibit moderate binding

Scheme 4[a]

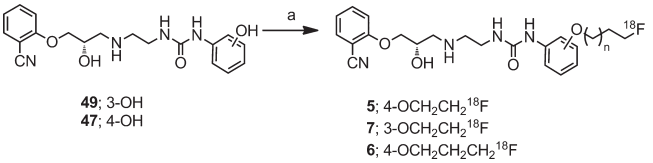

[a] Reagent and conditions: (a) Compound **41** or **62**, K_2CO_3, MeCN, 95 °C, 20 min.

Table 1. Fluorinated Analogues of ICI 89,406 (1) and OMe-ICI 89,406 (2)

compound	β_1[a]	β_2/β_1	cLogD
A_1-B_1 (**2**)	0.11	145	0.85
A_1-B_2 (**3**)	0.2	69	0.57
A_1-B_3 (**4**)	0.1	150	1.23
A_1-B_4 (**5**)	0.08	448	1.05
A_1-B_5 (**6**)	0.25	65	1.42
A_1-B_6 (7)	*0.04*	*265*	*1.03*
A_1-B_7 (**8**)	1.5	13	0.39
A_2-B_8 (**9**)	21	164	−0.53
A_3-B_8 (**10**)	2	70	−1.87
A_1-B_9 (**11**)	1	511	−1.66
A_2-B_{10} (**12**)	2	32	2.07
A_1-B_{11} (**13**)	0.1	50	0.92
A_1-B_{12} (**14**)	0.3	345	0.19
A_1-B_{13} (**15**)	0.05	723	0.86
A_1-B_{14} (16)	*0.05*	*>1000*	*0.47*
A_1-B_{15} (**17**)	0.35	163	0.35
A_1-B_{16} (**18**)	26	8	1.04
A_1-B_{17} (**19**)	10	10	−0.13
A_1-B_{18} (**20**)	>100	0.05	−0.59
A_1-B_{19} (**21**)	20	4	−0.74
A_1-B_{20} (**22**)	10	4	0.92
A_1-B_{21} (**23**)	3	30	0.42
A_1-B_{22} (**24**)	0.14	6	1.28
A_1-B_{23} (**25**)	5	0.1	0.91

[a] IC_{50} values are expressed in nanomolar concentrations.

potency to β_1-AR (IC_{50} = 21 and 2 nM, respectively), while maintaining good β_1/β_2-AR selectivity (164- and 70-fold, respectively; Table 1). Transposing the fluorine atom from the A region to the B region (**11**) once again resulted in a significant increase in β_1-AR binding activity and selectivity as compared to **9** and **10**. Although compounds **9**−**11** were comparable in their selectivity profile to **3**−**7**, the β_1-AR binding potency was approximately 10-fold lower.

Despite numerous reports of β_1-AR ligands that contain an aryloxy propanolamine pharmacophore, many of these compounds are in fact not selective for β_1-AR.[28] Considering **5**−**7** contain both the aryloxy propanolamine backbone and a urea-substituted aromatic system (B region), one may conclude that the enhanced β_1-AR potency and selectivity is in fact attributed to these additional structural features. As such, supplemental structure−activity relationship (SAR) studies were conducted to evaluate structural requirements within the aryloxy propanolamine backbone of ligands **5**−**7** necessary to maintain potency

dx.doi.org/10.1021/ml1002458 |*ACS Med. Chem. Lett.* 2011, 2, 650–655

Table 2. Biodistribution of [^{18}F]-ICI 89,406 Analogues in Rats[a,b]

organ	[^{18}F]**5**[b]	[^{18}F]**6**[a]	[^{18}F]**7**[b]
blood	0.18 ± 0.07	0.21 ± 0.01	0.14 ± 0.05
heart	0.48 ± 0.16	0.42 ± 0.15	0.62 ± 0.03
lung	0.97 ± 0.26	0.63 ± 0.27	0.79 ± 0.11
liver	1.14 ± 0.33	1.03 ± 0.52	1.14 ± 0.12
spleen	0.37 ± 0.02	0.40 ± 15	0.52 ± 0.09
kidney	1.26 ± 0.29	1.38 ± 0.16	2.01 ± 0.21
femur	0.27 ± 0.05	0.63 ± 0.16	0.16 ± 0.01
muscle	0.08 ± 0.02	0.09 ± 0.01	0.10 ± 0.01

[a] Data are expressed as the % ID/g ± SD with three animals per data point at 30 min postinjection. [b] Data are expressed as the % ID/g ± SEM with two animals per data point at 30 min postinjection.

and selectivity. For example, introduction of a heteroatom in the B ring of parent structures **4** and **5** afforded the fluorinated pyridine derivatives **14** and **13**, respectively. Notably, **14** exhibited a 3-fold decrease in β_1-AR potency and a nearly 2-fold increase in β_1-AR selectivity as compared to **4**, while compound **13** maintained β_1-AR potency, albeit with markedly decreased selectivity as compared to **5**. Replacement of the fluorine atom in **14** with iodine or bromine yielded compounds **15** and **16**, which exhibited increased β_1-AR potency and selectivity; **15** and **16** may prove interesting structural targets as ^{124}I and ^{76}Br-labeled PET radiotracers.

Introduction of an additional nitrogen atom in the B ring of **16** generated a fluorinated pyrimidine analogue, which resulted in a minor decrease in β_1-AR potency and selectivity (**17**; IC_{50} = 0.35 nM; 163-fold), whereas replacement of the B ring with 5-membered heterocycles such as thiazole (**18**) or tetrazole (**19**) proved detrimental for both β_1-AR potency and selectivity. Not surprisingly, substitution of the B ring with saturated heterocycles as in **20** and **21** markedly decreased potency and selectivity and confirmed the aromatic structural requirements outlined above. A small structure−activity profile of the urea functionality within the linker connecting the A and B regions in **5**−**7** was also generated, where removal of either nitrogen atom within the urea functionality of **4** and **14** to afford the derived amides **24** and **23**, respectively, resulted in >10-fold decrease in both potency and selectivity. Replacement of the urea moiety with a sulfonamide linker (**25**) also proved detrimental. Overall, no improved functional groups were identified.

In summary, compounds **3**−**7**, **13**, and **14**, each containing a fluorine atom, exhibited β_1-AR binding (IC_{50} = 0.04−0.30 nM) and good receptor selectivity (50−450-fold) suitable for imaging studies. Our criteria for radioligand selection were the following: (a) β_1-binding affinity, <1 nM; (b) β_1/β_2 selectivity >50; (c) moderate cLogD values; and (d) readily labeled with fluorine-18. Compounds **5**−**7** were thus selected as representative candidates for labeling with fluorine-18 as they achieved our selection criteria, provided a range of activity and selectivity values, and maintained a cLogD value near one.

Biodistribution studies of [^{18}F]**5**−**7** in Sprague−Dawley (SD) rats are summarized in Table 2. In general, high extraction of the radiotracers from the blood pool into tissues such as heart, lung, and liver was observed at 30 min postinjection. Heart uptake of compounds [^{18}F]**5**−**7** was 0.48, 0.42, and 0.62% ID/g, at 30 min, with corresponding heart:lung ratios of 1:2, 1:1.5, and 1:1.27, respectively. Similar values were also observed between

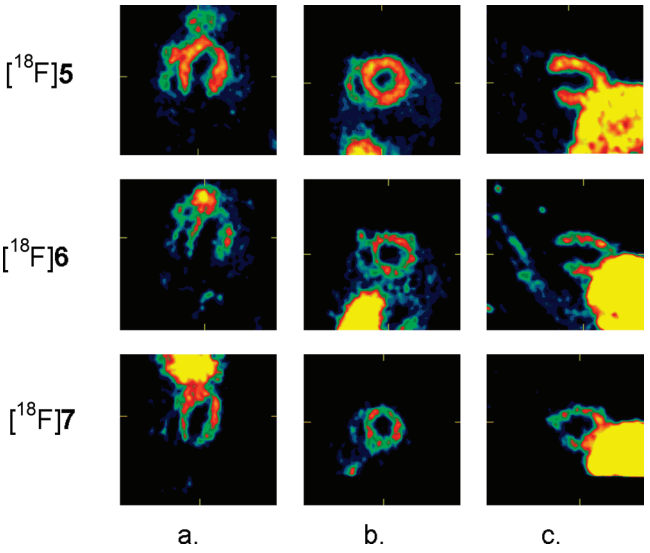

Figure 1. Images of the rat heart at 30 min. (a) Horizontal long axis, (b) short axis, and (c) vertical long axis.

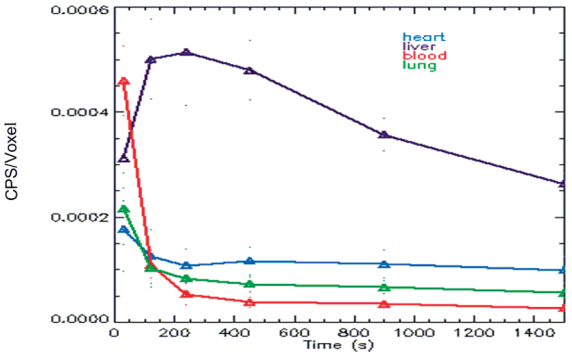

Figure 2. Time−activity curves from the imaging data of [^{18}F]**7**.

the heart and the liver. In these cases, uptake of radioligands [^{18}F]**5**−**7** appears unaffected by the position or length of the fluoroalkyl side chain.

Considering low expression of the β_1 receptor subtype, the observed preferential uptake of these tracers in lung tissue is likely nonspecific in nature. While this detail is consistent with the published literature,[20] several authors report challenges associated with the in vivo demonstration of subtype selectivity, including achieving a proper balance of specific activity and receptor occupancy as well as mediating the pharmacologic effects of preferred blocking agents (i.e., bradycardia from metaprolol). Despite achieving appropriate levels of specific activity in the present study, the observed tissue distribution will likely complicate future in vivo blocking studies.

Despite low statistical power, the abbreviated in vivo dissection studies outlined above help to establish gross differences in compound distribution and facilitate SAR development. More extensive, statistically relevant studies are however required, to distinguish subtle distribution differences and finalize lead candidate selection.

Dynamic PET imaging studies carried out on SD rats supported the biodistribution results. All three radiotracers were clearly visualized in both the myocardium and the liver at 30 min postinjection; however, at 60 min, significant wash-out of all

dx.doi.org/10.1021/ml1002458 |ACS Med. Chem. Lett. 2011, 2, 650–655

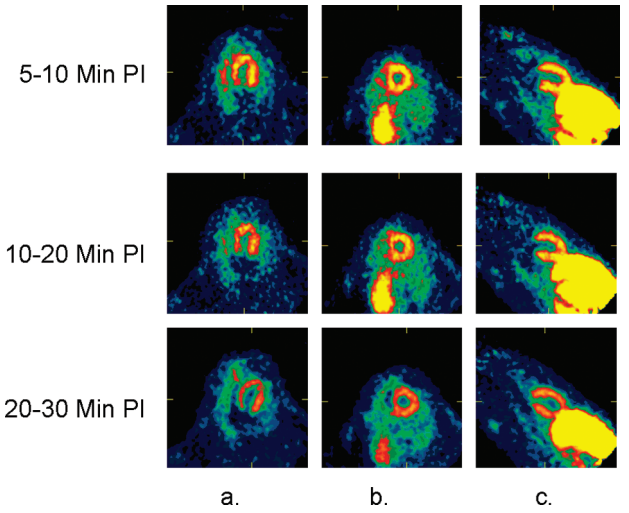

Figure 3. Images of [^{18}F]**7** in the rat heart at various time points. (a) Horizontal long axis, (b) short axis, and (c) vertical long axis.

three radiotracers was observed. Importantly, no interference from uptake in the lung was detected (Figure 1). In vivo metabolism study of [^{18}F]**7** revealed progressive loss of the parent species over time beginning at 83% and ending at 44% (2 and 30 min, respectively); a 30 min urine sample contained 76% of the parent species. Two unique metabolites were observed by HPLC analysis.

Considering the proximity of data derived from [^{18}F]**5**−**7**, compound [^{18}F]**7** was chosen as a representative example for more detailed in vivo evaluation. Time−activity plots generated through further study of [^{18}F]**7** showed rapid uptake of the radiotracer from the blood pool into the myocardium, lung, and liver <5 min postinjection, after which a steady level of the tracer was observed in blood, heart, and lung tissues as liver levels decreased markedly over time (Figure 2). Importantly, the time-dependent imaging study demonstrated [^{18}F]**7** does in fact accumulate in cardiac tissue within minutes after injection. Target:nontarget organ ratios remained relatively stable over time (Figure 3; Supporting Information).

In conclusion, multiple ^{18}F-labeled derivatives of the β_1-selective ligand ICI 89,406 were developed and evaluated as potential cardiac imaging tracers. An extensive structure−activity study identified a series of fluorine-substituted β_1-selective ligands, with potent β_1-AR affinity and β_1/β_2 selectivity. In vivo evaluation of [^{18}F]**5**−**7** in SD rats demonstrated uptake of the radiotracers in heart (0.48−0.62% ID/g), lung (0.63−0.97% ID/g), and liver (1.03−1.14% ID/g) tissue; results were confirmed through μPET imaging study.

Despite clear visualization of the myocardium, the considerable uptake of these tracers in nontarget tissues intimates a lack of specific binding, which may limit overall application of current imaging data and general utility of existing pharmacophore design. Future studies will attempt to reconcile these issues of selectivity and be directed toward decreasing liver uptake and improving overall cardiac retention.

■ ASSOCIATED CONTENT

Ⓢ Supporting Information. Full experimental procedures and characterization data for all new compounds described in this study. This material is available free of charge via the Internet at http://pubs.acs.org.

■ AUTHOR INFORMATION

Corresponding Author

*Tel: 978-671-8151. Fax 978-436-7500. E-mail: heike.radeke@lantheus.com.

■ REFERENCES

(1) Riemann, B.; Schaefers, M.; Law., M. P.; Wichter, T.; Schober, O. Radioligands for imaging myocardial α- and β-adrenoreceptors. *Nuklearmedizin* **2003**, *42*, 4–9.

(2) Brodde, O. E.; Bruck, H.; Leineweber, K. Cardiac Adrenoreceptors: Physiological and pathophysiological relevance. *J. Pharmacol. Sci.* **2006**, *100*, 323–337.

(3) Corr, P. B.; Crafford, W. A. Enhanced alpha-adrenergic responsiveness in ischemic myocardium: Role of alpha-adreergic blockade. *Am. Heart J.* **1981**, *102*, 605–612.

(4) Molenaar, P.; Parsonage, W. A. Fundamental considerations of beta-adrenoreceptor subtypes in human heart failure. *TRENDS Pharmacol. Sci.* **2005**, *26*, 368–375.

(5) de Jong, R. M.; Willemsen, T. M.; Slart, R. H. J.; Blanksma, P. K.; van Waarde, A.; Cornel, J. H.; Vaalburg, W.; van Veldhuisen, D. J.; Elsinga, P. H. Myocardial beta-adreoreceptor downregulation in idiopathic dilated cardiomyopathy measured in vivo with PET using the new radioligand (S)-[11C]CGP12388. *Eur. J. Nucl. Med. Mol. Imaging* **2005**, *32*, 443–447.

(6) Yamada, S.; Ishima, T.; Tomita, T.; Hatashi, T.; Okada, T.; Hayashi, E. Alterations in cardiac alpha and beta adrenoreceptors during the development of spontaneous hypertension. *J. Pharmacol. Exp. Ther.* **1984**, *228*, 454–459.

(7) Heusch, G. Alpha-adrenergic mechanisms in myocardial ischemia. *Circulation* **1990**, *81*, 1–13.

(8) Bergmann, S. R. Cardiac positron emission tomography. *Semin. Nucl. Med.* **1998**, *38*, 320–340.

(9) Kopka, K.; Schoeber, O.; Wagner, S. 18F-lablelled cardiac PET tracers: Selected probes for the molecular imaging of transporters, receptors and proteases. *Basic Res. Cardiol.* **2008**, *103*, 131–143.

(10) Kopka, K.; Law, M. P.; Breyholz, H.-J.; Faust, A.; Hoeltke, C.; Riemann, B.; Schober, O.; Schaefer, M.; Wagner, S. Non-invasive molecular imaging of beta-adrenoreceptors in vivo:Perspectives for PET-radioligands. *Curr. Med. Chem.* **2005**, *12*, 2057–2074.

(11) de Jong, R. M.; Blanksma, P. K.; van Waarde, A.; Veldhuisen, D. J. Measurement of myocardial beta-adrenoreceptos density in clinical studies: A role for positron emission tomography. *Eur. J. Nucl. Med.* **2002**, *29*, 88–97.

(12) Estes, N. A. M.; Weinstock, J.; Wang, P. J.; Homoud, M. K.; Link, M. S. Use of antiarrhythmics and implantable cardioverter-defibrillators in conjestive heart failure. *Am. J. Cardiol.* **2003**, *91*, 45–52.

(13) Momose, M.; Reder, S.; Raffel, D. M.; Watzlowik, P.; Wester, H.-J.; Nguyen, N.; Elsinga, P. H.; Bengel, F. M.; Remien, J.; Schwaiger, M. Evaluation of cardiac beta-adrenoreceptors in the isolated perfused rat heart using (S)-11C-CGP12388. *J. Nucl. Med.* **2004**, *45*, 471–477.

(14) Langer, O.; Halldin, C. PET and SPET tracers for mapping the cardiac nervous system. *Eur. J. Nucl. Med.* **2002**, *29*, 416–434.

(15) Schaefers, M.; Riemann, B.; Levkau, B.; Wichter, T.; Schaefer, K.; Kopka, K.; Breithardt; Schober, O. Current status and future application of cardiac receptor imaging with positron emission tomography. *Nucl. Med. Commun.* **2002**, *23*, 113–115.

(16) Majid, P. A.; Schreuder, J. E.; de Feyter, P. J.; Roos, J. P. Clinical, electrocardiographic, and hemodynamic effects of ICI89,406, a new cardioselective beta-adrenoreceptor antagonist with intrinsic sympathomimetic activity, in patients with angina pectoris. *J. Cardiovasc. Pharmacol.* **1980**, *2*, 435–444.

(17) Law, M. P.; Wagner, S.; Renner, C.; Pike, V. W.; Schober, O.; Schaefers, M. Preclinical evaluation of and 18F-labelled beta1-adrenoreceptor selective radioligand based on ICI89,406. *Nucl. Med. Biol.* **2010**, *37*, 517–526.

(18) Wagner, S.; Law, M. P.; Riemann, B.; Pike, V. W.; Breyholz, H.-J.; Hoeltke, C.; Faust, A.; Schober, O.; Schaefers, M.; Kopka, K. Synthesis of (*R*)- and (*S*)-[*O*-methyl-11C]*N*-[2-[3-(2-cyano-phenoxy)-2-hydroxy-propylamino]-ethyl]-*N*′-(4-methoxy-phenyl)-urea as candidate high affinity beta1-adrenoreceptor PET radioligands. *J. Labelled Compd. Radiopharm.* **2005**, *48*, 721–733.

(19) Kopka, K.; Wagner, S.; Riemann, B.; Law, M. P.; Puke, C.; Luthra, S. K.; Pike, V. W.; Wichter, T.; Schmitz, W.; Schober, O.; Schaefers, M. Design of new beta1-selective adrenoreceptor ligands as potential radioligands for in vivo imaging. *Bioorg. Med. Chem.* **2003**, *11*, 3513–3527.

(20) Law, M. P.; Wagner, S.; Kopka, K.; Pike, V. W.; Schober, O.; Schaefers, M. Are [O-methyl-11C]derivatives of ICI 89,406 beta1-adrenoreceptor selective radioligands suitable for PET? *Eur. J. Nucl. Med. Mol. Imaging* **2008**, *35*, 174–185 and references therein.

(21) Purohit, A.; Harris, T. Robinson, S. P.; Yalamanchili, P.; Azure, M. T.; Casebier, S. D. Preparation of [18F]containing phenylether derivatives as cardiac beta1 adrenoreceptor ligands for imaging congestive heart failure. WO 2008/083054A2.

(22) Radeke, H. S.; Purohit, A.; Harris, T. D.; Hansen, K.; Broekema, M.; Hu, C.; Jones, R.; Azure, M.; Cdebaca, M.; Yalamanchili, P. Synthesis and evaluation of fluorinated beta1-adrenoreceptor selective ligands Abstract of Papers, 240th ACS National Meeting, Boston, MA, USA, August 22−26, 2010.

(23) Pence, M.; Mee, H. T.; Chang, G. Enhanced chemoselective aminolysis of epoxides using diethylmethoxyborane, Abstracts of Papers, 230th ACS National Meeting, August 28−September 1, 2005.

(24) Musachio, J. L. Radiosynthesis and reactivities of novel [18F]2-fluoroethyl arylsulfonates. *J. Labelled Compd. Radiopharm.* **2005**, *48*, 735–747.

(25) Zuhayra, M. New approach for the synthesis of [18F] fluoroethyltyrosine for cancer imaging: Simple, fast, and high yielding automated synthesis. *Bioorg. Med. Chem.* **2009**, *17*, 7441–7448.

(26) Wagner, S.; Law, M. P.; Riemann, B.; Pike, V. W.; Breyholz, H.-J.; Hoeltke, C.; Faust, A.; Renner, C.; Schober, O.; Schaefers, M.; Kopka, K. Synthesis of and 18F-labeled high affinity beta1-adrenoreceptor PET radioligand based on ICI 89,406. *J. Labelled Compd. Radiopharm.* **2006**, *49*, 177–195.

(27) Wagner, S.; Kopka, K.; Law, M. P.; Riemann, B.; Pike, V. W.; Schober, O.; Schaefers, M. Synthesis and first in vivo evaluation of new selective high affinity beta1-adrenoreceptor radioligands for SPECT based on ICI 89, 406. *Bioorg. Med. Chem.* **2004**, *12*, 4117–4132.

(28) Large, M. S.; Smith, L. H. *J. Med. Chem.* **1982**, *25*, 1286–1292.